Asian Journal of Chemistry; Vol. 35, No. 9 (2023), 2092-2102

ASIAN JOURNAL OF CHEMISTRY

https://doi.org/10.14233/ajchem.2023.28081

Synthesis, Characterization, Biological Evaluation, DFT Studies and Molecular Docking of Novel 12-(2-(1*H*-Imidazol-1-yl)quinolin-3-yl)-8-methyl-2,3,4,12-tetrahydro-1*H*-benzo[4,5]thiazolo[2,3-*b*]quinazolin-1-one and its Derivatives

PUJA SHARMA[1,*], RAJAT PATEL[1], ROHIT R. KOSHTI[1], AKSHAY VYAS[1] and CHETAN B. SANGANI[2]

[1]Shri Maneklal M. Patel Institute of Sciences & Research, Kadi Sarva Vishwavidyalaya, Gandhinagar-382024, India
[2]Department of Chemistry, Government Science College, Sector-15, Gandhinagar-382016, India

*Corresponding author: E-mail: madhav10722@gmail.com; chetansangani1986@yahoo.com

Received: 1 June 2023; *Accepted*: 4 July 2023; *Published online*: 31 August 2023; AJC-21348

Twelve new compounds were synthesized consisting of biquinoline-imidazole-benzothiazole hybrids **6a-l** using a base catalyzed one pot MCR reaction, these were then screened for *in vitro* biological activities against cancer cell lines. Among the twelve prepared potential anticancer agents, compound **6j** was found to be the most active against EGFR (IC_{50} of 0.14 ± 0.03 µm), A549 and HepG2, also the same derivative of the series was found to be most active against FabH (IC_{50} of 3.1 µm) *E. coli*. Further, the molecules were analyzed for DFT and molecular docking studies to calculate the distance and angle between the active parts of the molecules as well as charge density distribution over the molecules, which provides a qualitative measure for the effective the binding of molecules in the active pockets with greater binding affinity.

Keywords: EGFR, FabH, DFT, Computational analysis, Active pockets, *in vitro* biological activities.

INTRODUCTION

Despite the significant research and exceptional growth in medicinal chemistry for the treatment of cancer [1], it is still known to be a serious public health problem worldwide and is the second leading cause of death [2]. The most widely used treatments for cancer apart from surgery includes radiation therapy and chemotherapy [3]. One important chemotherapy method to prevent the growth and spread of cancer cells is target therapy which involves targeting specific genes or proteins [4,5]. EGFR is a glycoprotein, which is primarily responsible for providing pathways for the cell proliferation, angiogenesis, apoptosis and metastatic spread [6,7]. Overexpression of EGFR is reported in different types of tumors and this critical role of EGFR in the cell signalling pathway has contributed significantly in the new discoveries for cancer treatment [8,9]. Also, excessive use of antibiotics has led to the drug resistance by certain bacteria and poses a serious threat to the health care sector, which has led to the need for novel therapeutics [10-13]. So, focus is now on finding new antimicrobial agents, which can overcome these problems faced by the medical fraternity. Fatty acid biosynthesis (FAS II) is a biochemical pathway that is emerging as a major target for the development of novel antibacterial agents [14-16]. One of the crucial enzyme within this pathway is β-ketoacyl-acyl carrier protein synthase III (FabH) has significant importance due to its role in catalyzing the earliest stages of fatty acid synthesis (FAS), which is responsible for the bacterial survival, highlighting the significance of FabH. Hence, FabH presents an effective route for the designing of novel antimicrobial agents [17,18].

Nitrogen and sulphur containing heterocyclic compounds are an important class of organic compounds because of their wide occurrence in nature as well as because of their varied biological activities [19]. Due to their ability to interact with enzyme binding pockets and block the biological pathways linked to tumor growth, they act as an excellent choice in designing anticancer drugs [20,21]. Also, they can be further modified with additional substituents easily and cover a broad area in medical research, which leads to a pivotal role in new drug discovery. Quinoline or benzo[*b*]pyridine is known to be one of the most important *N*-containing heterocyclic scaffolds due to its exceptional biological activities like anticancer, antifungal,

antiasthmatic, antibacterial, antimalarial, anticonvulsant, anti-inflammatory *etc*. [22-26]. Quinoline and imidazole are known to exhibit excellent anticancer activities [27,28] and can be used in designing new anticancer drugs along with several pharmacophores. One such pharmacophore used in this study is benzothiazole as it is known to possess significant anticancer [29,30] and antimicrobial activities [30-33].

The significant biological importance of these heterocyclic moieties was taken into consideration in the molecular designing and one-pot multicomponent reaction (MCR) was involved to carry out the synthesis of a series of 12 biquinoline derivatives containing imidazole-benzothiazole scaffolds followed by their characterization and biological evaluation for any significant importance. DFT studies and molecular docking was also done for the same. Keeping in mind the significant antimicrobial properties of three biologically active compounds, in present work, synthesis, characterization, biological evaluation, DFT studies and molecular docking of novel 12-(2-(1*H*-imidazol-1-yl)quinolin-3-yl)-8-methyl-2,3,4,12-tetrahydro-1*H*-benzo[4,5]thiazolo[2,3-*b*] quinazolin-1-one and its derivatives (**6a-l**) is reported using one pot MCR process.

EXPERIMENTAL

The reagents and solvents used were purchased commercially and used without further purification. The melting point (uncorrected) of the synthesized compounds **6a-l** were determined using XT4MP apparatus. Thin-layer chromatography (TLC) on aluminium plates coated with silica gel 60 F_{254}, 0.25 mm thickness, Merck was carried out to monitor each step. Mass spectra for all the synthesized compounds were scanned on a Thermo-fisher LCMS spectrometer. Perkin-Elmer CHN/S/O Elemental Analyzer 2400 Series II was used to carry out the elemental analysis. ^{1}H NMR and ^{13}C NMR spectra were recorded in DMSO-d_6 on a Bruker Avance 400 MHz spectrometer using TMS as the internal standard and DMSO as solvent. The IR spectra were recorded on Perkin Elmer spectrum-GX spectrophotometer using KBr pellets.

Synthesis of 2-chloroquinoline-3-carbaldehyde (1a-c): The required intermediates, 2-chloroquinoline-3-carbaldehyde **1a-c** were synthesized by Vilsmeier-Haack reaction (chloroformylation) as per the literature procedure (Meth-Cohn 1978) using acetanilide and its derivatives. Acetanilide and its derivatives were refluxed on a waterbath at 90 ºC for 6-7 h after adding to it calculated amount of DMF and $POCl_3$. The mixture was then poured on crushed ice with constant stirring when crude product got separated out in good yield (**Scheme-I**). The crude yellow precipitates were then filtered and washed with water thoroughly to remove all the acidic impurities. Finally, it was dried and recrystallized using ethyl acetate.

Synthesis of 2-(1*H*-imidazol-1-yl)quinoline-3-carbaldehyde (3a-c): Key intermediate, 2-(1*H*-imidazol-1-yl)quinoline-3-carbaldehyde (**3a-c**) was synthesized by refluxing equimolar amount of 2-chloroquinoline-3-carbaldehyde (**1a-c**) and imidazole (**2**) on a water bath in the presence of anhydrous K_2CO_3 in DMF at 85 ºC for 2 h. The resultant mixture after that was poured on crushed ice with stirring when the crude precipitates of the key intermediate separated out. It was neutralized with 1.5 N HCl and filtered, washed with water and dried and recrystallized using hot ethanol.

Synthesis of 12-(2-(1*H*-imidazol-1-yl)quinolin-3-yl)-8-methyl-2,3,4,12-tetrahydro-1*H*-benzo[4,5]thiazolo[2,3-*b*]-quinazolin-1-one (6a-l): The synthesis of the target molecules **6a-l** was carried out using a facile and efficient one pot three-component MCR reaction between the key intermediate, 2-(1*H*-imidazol-1-yl)quinoline-3-carbaldehyde (**3a-c**), 6-methylbenzo[*d*]thiazol-2-amine or 6-methoxybenzo[*d*]thiazol-2-amine (**4a-b**) and cyclohexane-1,3-dione (**5a-b**) in an round bottom flask using ethanol as solvent and a catalytic amount of piperidine (**Scheme-I**). The mixture was refluxed for 2-3 h and on bringing it to room temperature, crude product separated out and finally recrystallized using ethanol.

12-(2-(1*H*-Imidazol-1-yl)quinolin-3-yl)-8-methyl-2,3,4,12-tetrahydro-1*H*-benzo[4,5]thiazolo[2,3-*b*]quinazolin-1-one (6a): Yield: 80%. IR (KBr, ν_{max}, cm^{-1}): 3005 (aromatic C-H

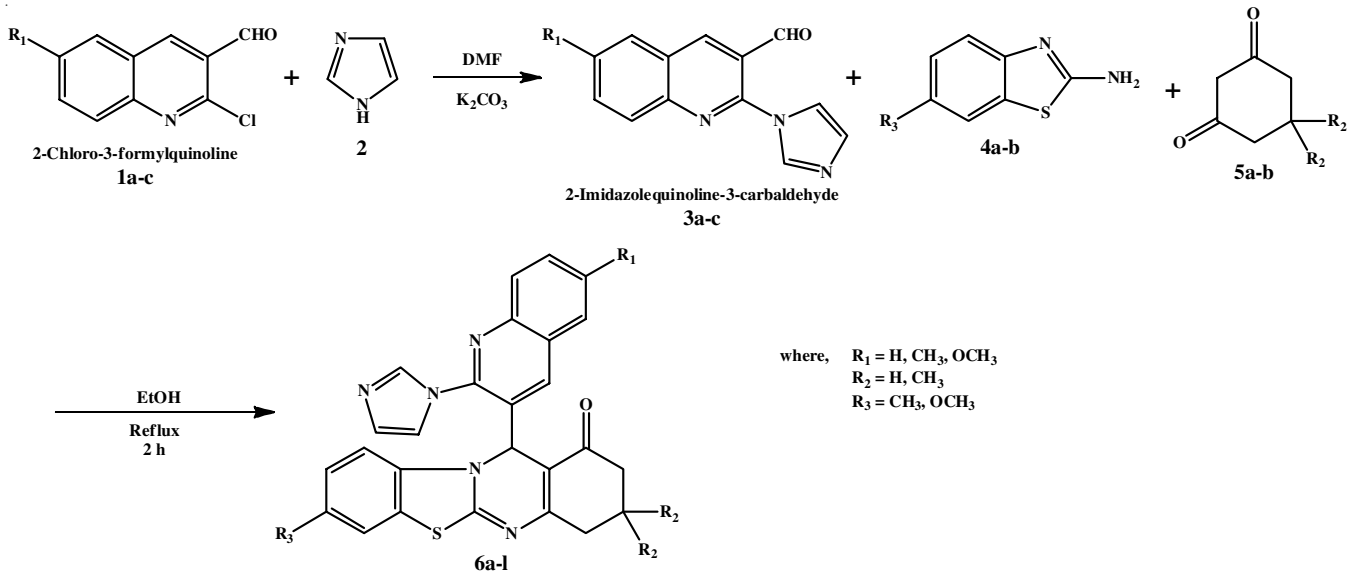

Scheme-I

str.), 1660 (C=O *str.*), 1569 & 1450 (C=C *str.* of aromatic ring), 1386 (C-N *str.*). ^{1}H NMR (400 MHz, DMSO-d_6) δ ppm: 2.36 (s, 3H, CH_3), 2.15 (p, 2H, -CH_2), 2.32 (t, 2H, -CH_2), 2.68 (t, 2H, -CH_2), 5.92 (s, 1H, -CH-), 7.08-7.90 (m, 11H, Ar-H). ^{13}C NMR (400 MHz, DMSO-d_6) δ ppm: 18.40 (CH_3), 18.65, 29.20, 33.24 (CH_2), 62.50 (CH), 102.12, 106.93, 108.18, 114.35, 118.30, 119.56, 120.24, 121.00, 125.31, 130.00, 130.71, 132.45, 132.97, 135.56, 137.34, 139.62, 145.25, 146.15, 147.74, 155.21, 160.83 (Ar-C), 196.40 (C=O). MS (*m/z*): 463.15 (M^+). Anal. calcd. (found) % for $C_{27}H_{21}N_5OS$ (*m.w.* 463.56 g/mol): C, 69.96 (69.83); H, 4.57 (4.70); O, 3.45 (3.31); N, 15.11 (15.24); S, 6.92 (7.05).

12-(2-(1*H*-Imidazol-1-yl)quinolin-3-yl)-8-methoxy-2,3,4,12-tetrahydro-1*H*-benzo[4,5]thiazolo[2,3-*b*]quinazolin-1-one (6b): Yield: 77%. IR (KBr, ν_{max}, cm^{-1}): 3006 (aromatic C-H *str.*), 1662 (C=O *str.*), 1569 & 1450 (C=C *str.* of aromatic ring), 1386 (C-N *str.*), 1238 & 1045 (C-O-C asym & sym *str.* of -OCH_3). ^{1}H NMR (400 MHz, DMSO-d_6) δ ppm: 2.15 (p, 2H, -CH_2), 2.32 (t, 2H, -CH_2), 2.68 (t, 2H, -CH_2), 3.78 (s, 3H, OCH_3), 5.92 (s, 1H, -CH-), 6.92-7.90 (m, 11H, Ar-H). ^{13}C NMR (400 MHz, DMSO-d_6) δ ppm: 18.65, 29.20, 33.24 (CH_2), 54.80 (OCH_3), 62.50 (CH), 102.12, 106.93, 108.18, 114.35, 118.30, 119.56, 121.05, 122.00, 125.31, 130.00, 131.80, 132.45, 133.50, 135.56, 137.34, 141.10, 145.25, 146.15, 147.74, 155.21, 160.83 (Ar-C), 196.40 (C=O). MS (*m/z*): 479.14 (M^+). Anal. calcd. (found) % for $C_{27}H_{21}N_5O_2S$ (*m.w.* 479.56 g/mol): C, 67.62 (67.48); H, 4.41 (4.58); O, 6.67 (6.45); N, 14.60 (14.65); S, 6.69 (6.60).

12-(2-(1*H*-Imidazol-1-yl)quinolin-3-yl)-3,3,8-trimethyl-2,3,4,12-tetrahydro-1*H*-benzo[4,5]thiazolo[2,3-*b*]quinazolin-1-one (6c): Yield: 81%. IR (KBr, ν_{max}, cm^{-1}): 3005 (aromatic C-H *str.*), 1665 (C=O *str.*), 1565 & 1445 (C=C *str.* of aromatic ring), 1386 (C-N *str.*). ^{1}H NMR (400 MHz, DMSO-d_6) δ ppm: 1.92 (s, 3H, CH_3), 1.97 (s, 3H, CH_3), 2.36 (s, 3H, CH_3), 2.12 (s, 2H, -CH_2), 2.52 (s, 2H, -CH_2), 5.92 (s, 1H, -CH-), 7.02-7.88 (m, 11H, Ar-H). ^{13}C NMR (400 MHz, DMSO-d_6) δ ppm: 18.40, 23.20, 23.25 (CH_3), 28.12 (C), 38.20, 48.44 (CH_2), 62.50 (CH), 102.12, 106.70, 108.18, 114.35, 118.78, 119.56, 120.24, 120.45, 125.31, 130.00, 131.31, 132.45, 132.97, 135.56, 137.34, 139.62, 145.25, 146.15, 148.00, 155.21, 160.83 (Ar-C), 196.40 (C=O). MS (*m/z*): 491.18 (M^+). Anal. calcd. (found) % for $C_{29}H_{25}N_5OS$ (*m.w.* 491.61 g/mol): C, 70.85 (70.71); H, 5.13 (5.27); O, 3.25 (3.34); N, 14.25 (14.11); S, 6.52 (6.38).

12-(2-(1*H*-Imidazol-1-yl)quinolin-3-yl)-8-methoxy-3,3-dimethyl-2,3,4,12-tetrahydro-1*H*-benzo[4,5]thiazolo[2,3-*b*]quinazolin-1-one (6d): Yield: 75%. IR (KBr, ν_{max}, cm^{-1}): 3008 (aromatic C-H *str.*), 1662 (C=O *str.*), 1565 & 1445 (C=C *str.* of aromatic ring), 1388 (C-N *str.*), 1240 & 1043 (C-O-C asym & sym *str.* of -OCH_3). ^{1}H NMR (400 MHz, DMSO-d_6) δ ppm: 1.92 (s, 3H, CH_3), 1.97 (s, 3H, CH_3), 2.12 (s, 2H, -CH_2), 2.52 (s, 2H, -CH_2), 3.78 (s, 3H, OCH_3), 5.92 (s, 1H, -CH-), 6.92-7.90 (m, 11H, Ar-H). ^{13}C NMR (400 MHz, DMSO-d_6) δ ppm: 23.20, 23.25 (CH_3), 28.12 (C), 38.20, 48.44 (CH_2), 54.80 (OCH_3), 62.50 (CH), 102.12, 106.70, 108.18, 114.35, 118.78, 119.56, 120.24, 120.45, 125.31, 130.00, 131.31, 132.45, 132.97, 135.56, 137.34, 139.62, 145.25, 146.15, 148.00, 155.21, 160.83 (Ar-C), 196.40 (C=O). MS (*m/z*): 507.17 (M^+). Anal. calcd. (found) % for $C_{29}H_{25}N_5O_2S$ (*m.w.* 507.61 g/mol): C, 68.62 (68.75); H, 4.96 (5.08); O, 6.30 (6.21); N, 13.80 (13.68); S, 6.32 (6.44).

12-(2-(1*H*-Imidazol-1-yl)-6-methylquinolin-3-yl)-8-methyl-2,3,4,12-tetrahydro-1*H*-benzo[4,5]thiazolo[2,3-*b*]-quinazolin-1-one (6e): Yield: 82%. IR (KBr, ν_{max}, cm^{-1}): 3006 (aromatic C-H *str.*), 1665 (C=O *str.*), 1569 & 1450 (C=C *str.* of aromatic ring), 1385 (C-N *str.*). ^{1}H NMR (400 MHz, DMSO-d_6) δ ppm: 2.36 (s, 3H, CH_3), 2.45 (s, 3H, CH_3), 2.15 (p, 2H, -CH_2), 2.32 (t, 2H, -CH_2), 2.68 (t, 2H, -CH_2), 5.92 (s, 1H, -CH-), 7.08-7.90 (m, 10H, Ar-H). ^{13}C NMR (400 MHz, DMSO-d_6) δ ppm: 18.40, 19.85 (CH_3), 18.65, 29.20, 33.24 (CH_2), 62.50 (CH), 102.12, 106.93, 108.18, 114.35, 118.30, 119.56, 120.24, 121.00, 125.31, 130.00, 130.71, 132.45, 132.97, 135.56, 137.34, 139.62, 145.25, 146.15, 147.74, 155.21, 160.83 (Ar-C), 196.40 (C=O). MS (*m/z*): 477.16 (M^+). Anal. calcd. (found) % for $C_{28}H_{23}N_5OS$ (*m.w.* 477.59 g/mol): C, 70.42 (70.35); H, 4.85 (4.98); O, 3.35 (3.50); N, 14.66 (14.47); S, 6.71 (6.58).

12-(2-(1*H*-Imidazol-1-yl)-6-methylquinolin-3-yl)-8-methoxy-2,3,4,12-tetrahydro-1*H*-benzo[4,5]thiazolo[2,3-*b*]-quinazolin-1-one (6f): Yield: 76%. IR (KBr, ν_{max}, cm^{-1}): 3005 (aromatic C-H *str.*), 1663 (C=O *str.*), 1569 & 1450 (C=C *str.* of aromatic ring), 1387 (C-N *str.*), 1237 & 1043 (C-O-C asym & sym *str.* of -OCH_3). ^{1}H NMR (400 MHz, DMSO-d_6) δ ppm: 2.45 (s, 3H, CH_3), 2.15 (p, 2H, -CH_2), 2.32 (t, 2H, -CH_2), 2.68 (t, 2H, -CH_2), 3.78 (s, 3H, OCH_3), 5.92 (s, 1H, -CH-), 6.92-7.90 (m, 10H, Ar-H). ^{13}C NMR (400 MHz, DMSO-d_6) δ ppm: 19.85 (CH_3), 18.65, 29.20, 33.24 (CH_2), 54.80 (OCH_3), 62.50 (CH), 102.12, 106.93, 108.18, 114.35, 118.30, 119.56, 120.24, 120.71, 125.31, 130.00, 130.71, 131.25, 132.97, 134.50, 136.34, 139.62, 145.25, 146.15, 148.24, 155.21, 160.83 (Ar-C), 196.40 (C=O). MS (*m/z*): 493.16 (M^+). Anal. calcd. for $C_{28}H_{23}N_5O_2S$ (493.59 g/mol): C, 68.14 (68.27); H, 4.70 (4.81); O, 6.48 (6.32); N, 14.19 (14.32); S, 6.50 (6.43).

12-(2-(1*H*-Imidazol-1-yl)-6-methylquinolin-3-yl)-3,3,8-trimethyl-2,3,4,12-tetrahydro-1*H*-benzo[4,5]thiazolo[2,3-*b*]quinazolin-1-one (6g): Yield: 80%. IR (KBr, ν_{max}, cm^{-1}): 3007 (aromatic C-H *str.*), 1666 (C=O *str.*), 1564 & 1443 (C=C *str.* of aromatic ring), 1385 (C-N *str.*). ^{1}H NMR (400 MHz, DMSO-d_6) δ ppm: 1.92 (s, 3H, CH_3), 1.97 (s, 3H, CH_3), 2.36 (s, 3H, CH_3), 2.45 (s, 3H, CH_3), 2.12 (s, 2H, -CH_2), 2.52 (s, 2H, -CH_2), 5.92 (s, 1H, -CH-), 6.92-7.95 (m, 10H, Ar-H). ^{13}C NMR (400 MHz, DMSO-d_6) δ ppm: 18.40, 19.85, 23.20, 23.25 (CH_3), 28.12 (C), 38.20, 48.44 (CH_2), 62.50 (CH), 102.12, 106.70, 108.18, 114.35, 119.00, 119.56, 120.24, 120.45, 125.31, 130.00, 130.92, 132.45, 133.35, 135.56, 137.34, 140.22, 145.25, 146.15, 148.00, 155.21, 160.83 (Ar-C), 196.40 (C=O). MS (*m/z*): 505.19 (M^+). Anal. calcd. (found) % for $C_{30}H_{27}N_5OS$ (*m.w.* 505.64 g/mol): C, 71.26 (71.12); H, 5.38 (5.24); O, 3.16 (3.30); N, 13.85 (13.93); S, 6.34 (6.21).

12-(2-(1*H*-Imidazol-1-yl)-6-methylquinolin-3-yl)-8-methoxy-3,3-dimethyl-2,3,4,12-tetrahydro-1*H*-benzo-[4,5]thiazolo[2,3-*b*]quinazolin-1-one (6h): Yield: 80%. IR (KBr, ν_{max}, cm^{-1}): 3005 (aromatic C-H *str.*), 1663 (C=O *str.*), 1565 & 1445 (C=C *str.* of aromatic ring), 1384 (C-N *str.*), 1235 & 1044 (C-O-C asym & sym *str.* of -OCH_3). ^{1}H NMR (400 MHz, DMSO-d_6) δ ppm: 1.92 (s, 3H, CH_3), 1.97 (s, 3H, CH_3), 2.45 (s, 3H, CH_3),

2.12 (s, 2H, -CH_2), 2.52 (s, 2H, -CH_2), 3.78 (s, 3H, OCH_3), 5.92 (s, 1H, -CH-), 6.92-7.90 (m, 10H, Ar-H). ^{13}C NMR (400 MHz, DMSO-d_6) δ ppm: 19.85, 23.20, 23.25 (CH_3), 28.12 (C), 38.20, 48.44 (CH_2), 54.80 (OCH_3), 62.50 (CH), 102.12, 106.70, 108.18, 114.35, 119.00, 119.56, 120.24, 120.45, 125.31, 130.00, 130.92, 132.45, 133.35, 135.56, 137.34, 140.22, 145.25, 146.15, 148.00, 155.21, 160.83 (Ar-C), 196.40 (C=O). MS (*m/z*): 521.19 (M^+). Anal. calcd. (found) % for $C_{30}H_{27}N_5O_2S$ (*m.w.* 521.64 g/mol): C, 69.08 (69.20); H, 5.22 (5.12); O, 6.13 (6.25); N, 13.43 (13.25); S, 6.15 (6.23).

12-(2-(1*H*-Imidazol-1-yl)-6-methoxyquinolin-3-yl)-8-methyl-2,3,4,12-tetrahydro-1*H*-benzo[4,5]thiazolo[2,3-*b*]-quinazolin-1-one (6i): Yield: 78%. IR (KBr, ν_{max}, cm^{-1}): 3008 (aromatic C-H *str.*), 1665 (C=O *str.*), 1566 & 1448 (C=C *str.* of aromatic ring), 1385 (C-N *str.*), 1236 & 1046 (C-O-C asym & sym *str.* of -OCH_3). ^{1}H NMR (400 MHz, DMSO-d_6) δ ppm: 2.36 (s, 3H, CH_3), 2.15 (p, 2H, -CH_2), 2.32 (t, 2H, -CH_2), 2.68 (t, 2H, -CH_2), 3.81 (s, 3H, OCH_3), 5.92 (s, 1H, -CH-), 7.10-7.98 (m, 10H, Ar-H). ^{13}C NMR (400 MHz, DMSO-d_6) δ ppm: 18.40 (CH_3), 18.65, 29.20, 33.24 (CH_2), 54.80 (OCH_3), 62.50 (CH), 102.12, 106.93, 108.70, 114.35, 118.30, 119.56, 120.24, 120.80, 125.31, 129.58, 130.71, 132.45, 132.97, 135.56, 137.34, 139.62, 144.83, 146.15, 148.41, 155.21, 160.83 (Ar-C), 196.40 (C=O). MS (*m/z*): 493.16 (M^+). Anal. calcd. (found) % for $C_{28}H_{23}N_5O_2S$ (*m.w.* 493.59 g/mol): C, 68.14 (68.29); H, 4.70 (4.52); O, 6.48 (6.31); N, 14.19 (14.31); S, 6.50 (6.37).

12-(2-(1*H*-Imidazol-1-yl)-6-methoxyquinolin-3-yl)-8-methoxy-2,3,4,12-tetrahydro-1*H*-benzo[4,5]thiazolo[2,3-*b*]quinazolin-1-one (6j): Yield: 76%. IR (KBr, ν_{max}, cm^{-1}): 3006 (aromatic C-H *str.*), 1663 (C=O *str.*), 1565 & 1446 (C=C *str.* of aromatic ring), 1384 (C-N *str.*), 1235 & 1044 (C-O-C asym & sym *str.* of -OCH_3). ^{1}H NMR (400 MHz, DMSO-d_6) δ ppm: 2.15 (p, 2H, -CH_2), 2.32 (t, 2H, -CH_2), 2.68 (t, 2H, -CH_2), 3.81 (s, 6h, 2×OCH_3), 5.92 (s, 1H, -CH-), 6.92-7.90 (m, 10H, Ar-H). ^{13}C NMR (400 MHz, DMSO-d_6) δ ppm: 18.65, 29.20, 33.24 (CH_2), 54.80 (2×OCH_3), 62.50 (CH), 102.12, 106.93, 108.70, 114.35, 118.30, 119.56, 120.24, 120.80, 125.31, 129.58, 130.71, 132.45, 132.97, 135.56, 137.34, 139.62, 144.83, 146.15, 148.41, 155.21, 160.83 (Ar-C), 196.40 (C=O). MS (*m/z*): 509.18 (M^+). Anal. calcd. (found) % for $C_{28}H_{23}N_5O_3S$ (*m.w.* 509.58 g/mol): C, 66.00 (66.12); H, 4.55 (4.68); O, 9.42 (9.28); N, 13.74 (13.56); S, 6.29 (6.42).

12-(2-(1*H*-Imidazol-1-yl)-6-methoxyquinolin-3-yl)-3,3,8-trimethyl-2,3,4,12-tetrahydro-1*H*-benzo[4,5]thiazolo[2,3-*b*]quinazolin-1-one (6k): Yield: 82%, IR (KBr, ν_{max}, cm^{-1}): 3007 (aromatic C-H *str.*), 1662 (C=O *str.*), 1564 & 1444 (C=C *str.* of aromatic ring), 1384 (C-N *str.*), 1235 & 1046 (C-O-C asym & sym *str.* of -OCH_3). ^{1}H NMR (400 MHz, DMSO-d_6) δ ppm: 1.92 (s, 3H, CH_3), 1.97 (s, 3H, CH_3), 2.36 (s, 3H, CH_3), 2.12 (s, 2H, -CH_2), 2.52 (s, 2H, -CH_2), 3.81 (s, 3H, OCH_3), 5.92 (s, 1H, -CH-), 6.92-7.88 (m, 10H, Ar-H). ^{13}C NMR (400 MHz, DMSO-d_6) δ ppm: 18.40, 23.20, 23.25 (CH_3), 28.12 (C), 38.20, 48.44 (CH_2), 54.80 (OCH_3), 62.50 (CH), 102.12, 106.70, 108.18, 113.75, 118.78, 120.00, 120.44, 121.34, 125.31, 130.00, 131.31, 132.24, 132.90, 135.56, 137.34, 139.62, 145.25, 146.15, 148.31, 155.21, 160.83 (Ar-C), 196.40 (C=O). MS (*m/z*): 521.19 (M^+). Anal. calcd. (found) % for $C_{30}H_{27}N_5O_2S$ (*m.w.* 521.64 g/mol): C, 69.08 (69.21); H, 5.22 (5.06); O, 6.13 (5.97); N, 13.43 (13.60); S, 6.15 (6.29).

12-(2-(1*H*-Imidazol-1-yl)-6-methoxyquinolin-3-yl)-8-methoxy-3,3-dimethyl-2,3,4,12-tetrahydro-1*H*-benzo[4,5]-thiazolo[2,3-*b*]quinazolin-1-one (6l): Yield: 76%. IR (KBr, ν_{max}, cm^{-1}): 3005 (aromatic C-H *str.*), 1663 (C=O *str.*), 1565 & 1445 (C=C *str.* of aromatic ring), 1384 (C-N *str.*), 1235 & 1044 (C-O-C asym & sym *str.* of -OCH_3). ^{1}H NMR (400 MHz, DMSO-d_6) δ ppm: 1.92 (s, 3H, CH_3), 1.97 (s, 3H, CH_3), 2.12 (s, 2H, -CH_2), 2.52 (s, 2H, -CH_2), 3.81 (s, 6h, 2×OCH_3), 5.92 (s, 1H, -CH-), 6.92-7.90 (m, 10H, Ar-H). ^{13}C NMR (400 MHz, DMSO-d_6) δ ppm: 23.20, 23.25 (CH_3), 28.12 (C), 38.20, 48.44 (CH_2), 54.80 (2×OCH_3), 62.50 (CH), 102.12, 106.70, 109.00, 114.35, 119.21, 120.12, 120.64, 121.34, 125.31, 130.43, 131.43, 132.45, 133.35, 135.56, 137.34, 140.22, 145.25, 146.15, 148.00, 155.21, 160.83 (Ar-C), 196.40 (C=O). MS (*m/z*): 537.18 (M^+). Anal. calcd. (found) % for $C_{30}H_{27}N_5O_3S$ (*m.w.* 537.64 g/mol): C, 67.02 (67.23); H, 5.06 (4.95); O, 8.93 (9.08); N, 13.03 (12.96); S, 5.96 (6.12).

RESULTS AND DISCUSSION

Spectral analysis: All the newly synthesized compounds **6a-l** were subjected to IR spectra to confirm the functional groups present in them. The IR spectra for carbonyl group (-CO) was observed in the range of 1666-1660 cm^{-1} for all **6a-l** synthesized compounds. Aromatic C-H stretching was observed in the region of 3008-3005 cm^{-1} while C=C stretching of the aromatic ring was found in the region of 1569-1450 cm^{-1}. A C-N stretching frequency was in the region of 1384-1388 cm^{-1}. A C-O-C asymmetric and symmetric stretching of methoxy (–OCH_3) group was observed for compounds **6b**, **6d**, **6f**, **6h**, **6i**, **6j**, **6k**, **6l** in the range of 1235-1240 and 1043-1046 cm^{-1} region.

The structure of all the synthesized compounds **6a-l** was further confirmed by carrying out ^{1}H NMR. A singlet for three protons of methyl group at R_1 substitution for compounds **6e**, **6f**, **6g**, **6h** appeared at δ 2.45 ppm and a singlet for three protons each in two methyl groups at R_2 substitution in compounds **6c**, **6d**, **6g**, **6h**, **6k**, **6l** was observed in the region of δ 1.92 and 1.97 ppm. NMR spectra as singlet for three protons for methyl group as R_3 substitution was observed at δ 2.46 ppm for compounds **6a**, **6c**, **6e**, **6g**, **6i**, **6k**. A pentet for two protons of the methylene group –CH_2 appeared in the region of δ 2.15 ppm and two triplets for two protons of the methylene group –CH_2 was observed at δ 2.32 and 2.68 ppm in compounds **6a**, **6b**, **6e**, **6f**, **6i**, **6j**. A singlet for two protons each for two methylene groups –CH_2 was observed at δ 2.12 and 2.52 ppm in compounds **6c**, **6d**, **6g**, **6h**, **6k**, **6l**. A singlet for an aromatic chiral proton appeared in the region of δ 5.92 ppm for all the synthesized compounds **6a-l** indicating the cyclization of the target product. A multiplet for aromatic protons ranging from ten to eleven in compounds **6a-l** was observed in the region of δ 6.92-7.90 ppm. A singlet for the three protons of the methoxy group at R_3 substitution resonated in the region of δ 3.78 ppm for compounds **6b**, **6d**, **6f**, **6h** whereas in compounds **6i**, **6k** a singlet for three protons as R_1 substitute of methoxy group appeared in the region of δ 3.81 ppm. In compounds **6j**, **6l** a

singlet for six protons of two methoxy groups was observed at δ 3.78 and 3.81 ppm.

To identify the nature of the carbon atoms all the synthesized compounds were analyzed for their ^{13}C NMR absorption spectra. The methyl group at R_1 substitution in compounds **6e**, **6f**, **6g**, **6h** showed signal in the range of δ 19.85 ppm while the methyl group as R_3 substitution in compounds **6a**, **6c**, **6e**, **6g**, **6i**, **6k** gave signal at δ 18.40 ppm. The presence of two methyl groups at R_2 substitution in compounds **6c**, **6d**, **6g**, **6h**, **6k**, **6l** showed signals at δ 23.20 and 23.25 ppm. The presence of methoxy group at R_1 and R_3 substitution in compounds **6b**, **6d**, **6f**, **6h**, **6i**, **6k**, **6l** was displayed by a single line at δ 54.80 ppm. A multiplet of aromatic carbon for compounds **6a-l** was confirmed in the range of δ 102.12-160.83 ppm. The presence of an aromatic carbonyl carbon atom in all compounds was displayed by a single peak at δ 196.40 ppm. The presence of methylene group in all the compounds **6a-l** was exhibited in the range of δ 18.65-48.44 ppm. Active methylene (C4) showed a single line at δ 62.50 ppm.

Biological evaluation

Antiproliferation and EGFR inhibitory activity: All the newly synthesized compounds having quinoline ring linked with imidazole from 2nd position and alkyl/alkoxy benzo[*d*]thiazole amine linked with cyclohexanone at 3rd position with various substitution matrix were tested for EGFR inhibitory activity as well as antiproliferation activity against known lung cancer cell line A549 known as adenocarcinoma human alveolar basal epithelial cell line and liver cancer cell line Hep G2. About EGFR inhibition, the mode of action to inhibit tyrosine kinase is well known, in short which is by stopping the transferring of signal between the two EGFR molecules. When the prepared molecules were tested for these activities, it was found that compound **6j** showed most potent activity amongst the synthesized compounds with IC_{50} of 0.14 ± 0.03 μM, while compounds **6k** and **6l** showed compared good activity with IC_{50} of 0.21 ± 0.04 μM and IC_{50} of 0.26 ± 0.02 μM, respectively (Table-1). In the case of antiproliferative activity against A549 and Hep G2 compounds **6k** and **6j** showed the most potent activity with IC_{50} of 2.21 ± 0.03 μM and 2.31 ± 0.04 μM, respectively, although compounds **6h**, **6j** and **6k** showed almost same potency against the A549 with IC_{50} of 2.21 ± 0.09 μM, 2.24 ± 0.04 μM and 2.21 ± 0.03 μM, while compound **6k** showed potency against the Hep G2 with IC_{50} of 2.98 ± 0.05 μM, although among all the prepared compounds only compound **6j** showed the nearest potency compared to the standard erlotinib.

TABLE-1
INHIBITION OF EGFR KINASE AND ANTIPROLIFERATIVE ACTIVITY IC_{50} (μM) OF COMPOUNDS **6a-l**

Compound	EGFR	A549	Hep G2
6a	3.81 ± 0.02	3.84 ± 0.03	3.97 ± 0.07
6b	3.27 ± 0.03	8.56 ± 0.14	9.21 ± 0.11
6c	8.25 ± 0.04	9.54 ± 0.12	11.27 ± 0.15
6d	3.77 ± 0.03	5.26 ± 0.11	6.31 ± 0.16
6e	6.24 ± 0.09	7.47 ± 0.08	7.69 ± 0.08
6f	4.98 ± 0.04	6.64 ± 0.07	7.21 ± 0.06
6g	9.61 ± 0.11	7.47 ± 0.05	5.47 ± 0.07
6h	1.61 ± 0.09	2.21 ± 0.09	4.38 ± 0.11
6i	5.21 ± 0.14	6.51 ± 0.05	7.51 ± 0.07
6j	0.14 ± 0.03	2.24 ± 0.04	2.31 ± 0.04
6k	0.21 ± 0.04	2.21 ± 0.03	2.98 ± 0.05
6l	0.26 ± 0.02	2.27 ± 0.04	3.34 ± 0.02
Erlotinib	0.032 ± 0.02	0.13 ± 0.01	0.12

***E. coli* FabH inhibitory activity:** The *E. coli* FabH inhibitory activity of the synthesized compounds **6a-l** were examined and their result as a concentration in micromole is represented in Table-2. Among the synthesized compounds, four showed a impartial inhibitory activity. Compound **6j** showed the most potent inhibitory activity with the IC_{50} of 3.1 μM, while compound **6g** showed inhibitory action at the IC_{50} of 3.3 μM, compound **6l** showed the IC_{50} of 3.8 μM and compound **6h** showed inhibitory action at the IC_{50} of 4.3 μM. While the other derivatives **6a**, **6b**, **6c**, **6d**, **6e**, **6f**, **6i** and **6k** showed relatively very low and poor inhibitory action at the IC_{50} of 17.5, 16.4, 8.2, 8.3, 13.1, 14.1, 16.7 and 8.7 μM, respectively.

TABLE-2
E. coli FabH INHIBITORY ACTIVITY OF SYNTHETIC COMPOUNDS **6a-l**

Compd.	R_1	R_2	R_3	*E. coli* FabH IC_{50} (μM)	Hemolysis $LC30^a$ (mg/mL)
6a	H	H	CH_3	17.5	> 10
6b	H	H	OCH_3	16.4	> 10
6c	H	CH_3	CH_3	8.2	> 10
6d	H	CH_3	OCH_3	8.3	> 10
6e	CH_3	H	CH_3	13.1	> 10
6f	CH_3	H	OCH_3	14.1	> 10
6g	CH_3	CH_3	CH_3	3.3	> 10
6h	CH_3	CH_3	OCH_3	4.3	> 10
6i	OCH_3	H	CH_3	16.7	> 10
6j	OCH_3	H	OCH_3	3.1	> 10
6k	OCH_3	CH_3	CH_3	8.7	> 10
6l	OCH_3	CH_3	OCH_3	3.8	> 10

[a]Lytic concentration 30%

Molecular docking study

With EGFR: The interaction of the prepared compounds with EGFR (PDB code: 1M17) was performed by docking the molecules with protein into the active pocket, to understand the behaviour of the pharmacophore with various substitutions allowing better fitting into the active pocket and can guide the SAR. The missing fragments and protonation correction in the protein PDB file was carried out using homology model preparation with assigning partial charge to the atoms using MOE software. The geometrically minimized energy structure of the ligand molecules were then docked at the ligand site with rigid receptor refinement, the resultant binding energy of all docked molecules are summarized in Table-3. From the output, it was observed that compound **6h** was bound into the active site of the EGFR pocket with the minimum binding energy of ΔG_b = -7.1517 kcal/mol, amongst the all docked, the 2D and 3D binding interaction with the pocket boundary and pocket cavity are shown in Fig. 1 with all the amino acid residues labelled with their short code within the radius of 4.5 Å of the ligand atom. Binding showed that compound **6h** bound in the site of EGFR through hydrophobic interaction. The

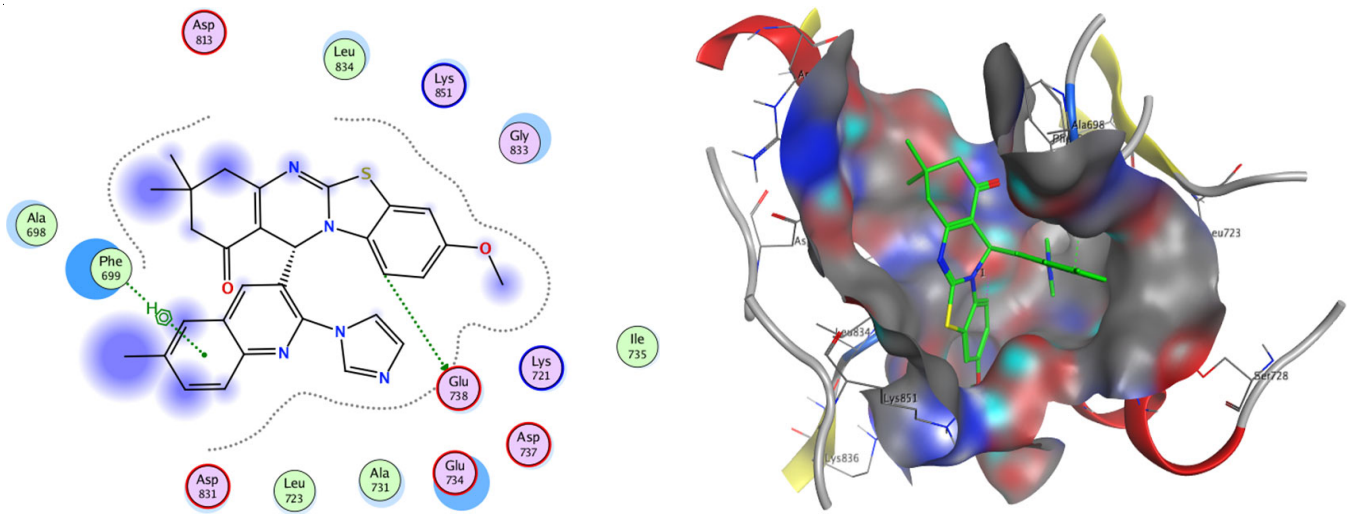

Fig. 1. 2D and 3D Binding model of compound **6h** into the active pocket of EGFR

TABLE-3
BINDING ENERGY OF SYNTHESIZED COMPOUNDS **6a-l** AND ERLOTINIB WITH EGFR AND FabH

Compd.	Binding energy (ΔG_b)	
	EGFR	FabH
6a	-6.6901	-6.8039
6b	-6.7903	-6.8095
6c	-6.1756	-7.3029
6d	-6.7982	-7.3515
6e	-6.6561	-7.0944
6f	-6.7163	-7.1541
6g	-6.6648	-7.4929
6h	-7.1517	-7.5574
6i	-6.7440	-7.2822
6j	-6.8219	-7.7221
6k	-7.1363	-7.3005
6l	-7.1030	-7.5376

binding was stabilized by two hydrogen bonds, among which one hydrogen bond formed between the hydrogen of the phenyl ring adjacent to thiazole ring and GLU738 with bond distance of 3.31 Å and second hydrogen bond between quinoline phenyl ring and Phe699 with bond distance of 3.59 Å in the form of arene hydrogen interaction. From this binding model, it could be concluded that these two hydrogen bonds from the quinoline and thaizolo with the pocket are can be said to be responsible for the effective EGFR inhibitory of compound **6j** from docking results.

With FabH: Similarly, to understand the behaviour of the pharmacophore with various substitutions allowing better fitting into the active pocket and to guide the SAR, molecular docking of the twelve prepared compounds and *E. coli* FabH was performed and examined on the binding model based on the *E. coli* FabH-CoA complex structure (PDB code: 1HNJ). A catalytic triad tunnel composed of Cys-His-Asn is found in the active site of the FabH, which is found in many of the bacteria. This triad which works as catalysis, plays an important role in the controlling of chain elongation as well as substrate binding and hence the alkyl chain of the CoA is broken at the Cys residue of the triad of FabH, the interaction occurring between the Cys and substrate seems to playing a significant role in the binding of the substrate. From the binding model of the studied twelve compounds, compound **6j** was found to be bound strongly into the active pocket of the FabH with the binding energy ΔG_b of -7.7221 kcal/mol on primary analysis of docking results. Binding affinity score of all the prepared compounds is represented in Table-3. The interactive binding model of compound **6j** with the active site of FabH protein in 2D and 3D model with the cavity boundary showed as dotted line and active pocket surface is depicted in Fig. 2. The binding between the pocket and ligand is formed through the hydrogen bonding and arene-arene interaction, where from the figure it can be seen that hydrogen bond is formed between the thiazole ring and the hydrogen of the GLY209 with bond distance of 4.37 Å, another arene hydrogen interaction is formed between the methoxy hydrogen and the pyrrole ring of indole of TRP32 with bond distance of 3.68 Å, the phenyl ring of the quinoline also forms arene-arene interaction with the TRP32, while the fourth interaction in the form of arene hydrogen interaction is formed between the nitrogen bearing quinoline ring and hydrogen of the GLY152 with bond distance of 3.53 Å. From this interaction and the binding score it can be primarily concluded that the strong hydrogen bonding by the quinoline fragment with GLY and TRP is responsible for the effective FabH inhibitory of compound **6j** in docking results.

Computational studies

Density functional theory: All the structures of twelve synthesized compounds were optimized to obtain the lowest possible energy level using quantum computational tool ORCA 5.0.3 with DFT method and B3LYP level of DFT theory and def-2SVP basis set [34]. The structure obtained with the lowest possible energy was then checked for their global minima by means of finding any negative vibrational frequency in IR range computationally with same parameters as used in case of optimization, hence finding no imaginary frequency value confirmed the acceptable geometry of compound at lowest single point energy. The computation study was performed with the aim of understanding the influence of change in substitution groups

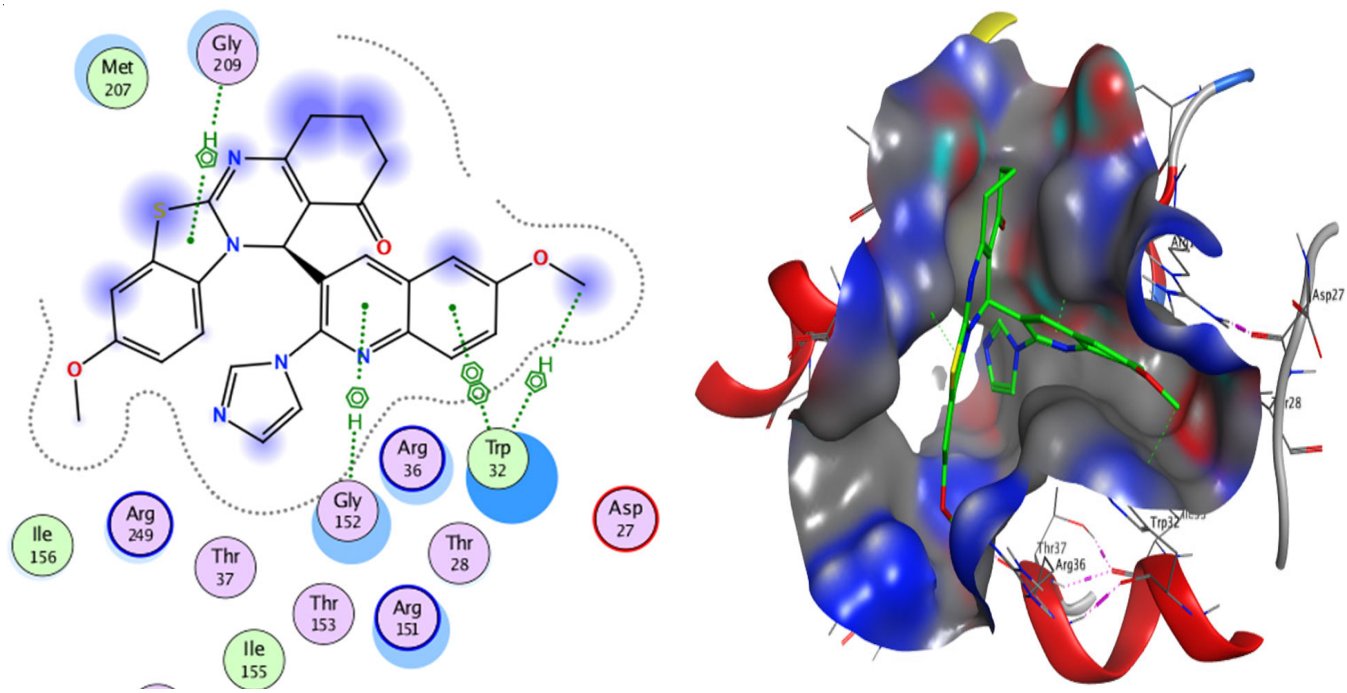

Fig. 2. 2D and 3D Binding model of compound **6j** into the active pocket of FabH

at R_1, R_2 and R_3 positions, These changes are thought to be changing the geometry of the molecule by changing the angle between the core of the planner groups affecting its shape ready to fit into the protein cavity and distribution of charge over the molecule as on individual atoms and their molecular orbital responsible for electronic properties of the molecule as they are good indicators of electron transport in the system, responsible for UV-vis properties of the molecule. As the linearity in the compound is composed of the three main fragments of the molecule, three imaginary planes were passed from the mole-

TABLE-4
FACTORS CALCULATED FROM THE QUANTUM COMPUTATIONAL DFT STUDY OF MOLECULES **6a-l**

Compound	Dipole moment (Debye)	Energy (a.u.)	Twist angle (θ)			E_{HOMO} (eV)	E_{LUMO} (eV)	$I = -E_{HOMO}$ (eV)	$A = -E_{LUMO}$ (eV)
			θ_1	θ_2	θ_3				
6a	6.036	-1786.70	32.50	67.73	89.06	-9.204	-3.933	9.204	3.933
6b	7.054	-1861.82	32.75	68.39	89.12	-9.027	-3.928	9.027	3.928
6c	6.109	-1865.23	42.00	57.38	87.89	-9.162	-3.955	9.162	3.955
6d	5.256	-1940.34	41.60	56.79	88.84	-8.997	-3.953	8.997	3.953
6e	7.257	-1825.96	39.37	70.05	88.69	-9.219	-3.754	9.219	3.754
6f	6.697	-1901.08	39.43	70.25	88.84	-9.070	-3.754	9.070	3.754
6g	7.224	-1904.48	39.49	70.05	88.91	-9.209	-3.755	9.209	3.755
6h	6.685	-1979.59	40.43	70.93	88.60	-9.065	-3.748	9.065	3.748
6i	8.174	-1901.08	39.03	69.25	88.66	-9.199	-3.580	9.199	3.580
6j	7.495	-1976.20	39.29	69.52	88.88	-9.060	-3.576	9.060	3.576
6k	8.156	-1979.60	41.03	70.35	88.11	-9.197	-3.565	9.197	3.565
6l	7.521	-2054.71	41.33	70.74	87.94	-9.059	-3.563	9.059	3.563

Compound	$\Delta E = I - A$ (eV)	$\eta = (I - A)/2$ (eV)	$\chi = (I - A)/2$ (eV)	$\sigma = 1/\eta$	$S = 1/2\eta$	$Pi = -\chi$	$\omega = (Pi)^2/2\eta$	$\Delta N_{max} = \chi/\eta$
6a	5.271	2.636	6.569	0.379	0.190	-6.569	8.185	2.492
6b	5.099	2.550	6.478	0.392	0.196	-6.478	8.229	2.541
6c	5.207	2.604	6.559	0.384	0.192	-6.559	8.261	2.519
6d	5.044	2.522	6.475	0.397	0.198	-6.475	8.312	2.567
6e	5.465	2.733	6.487	0.366	0.183	-6.487	7.699	2.374
6f	5.316	2.658	6.412	0.376	0.188	-6.412	7.734	2.412
6g	5.454	2.727	6.482	0.367	0.183	-6.482	7.704	2.377
6h	5.317	2.659	6.407	0.376	0.188	-6.407	7.719	2.410
6i	5.619	2.810	6.390	0.356	0.178	-6.390	7.266	2.274
6j	5.484	2.742	6.318	0.365	0.182	-6.318	7.279	2.304
6k	5.632	2.816	6.381	0.355	0.178	-6.381	7.230	2.266
6l	5.496	2.748	6.311	0.364	0.182	-6.311	7.247	2.297

cule, where first plane was passed from quinoline ring, the second plane was passed from the imidazole ring and the third plane was passed from benzothiazole ring. The angle between the R_1 substituted quinoline ring and the imidazole ring was noted as twist angle θ_1, the angle between the R_2 and R_3 substituted benzothiazole-quinoline core and imidazole ring was noted as twist angle θ_2, the angle between the R_1 substituted quinoline ring and the R_2 and R_3 substituted benzothiazole-quinoline core was noted as twist angle θ_3. It was conventional that, smaller the molecular orbital energy gap ΔE, the greater will be the reactivity and lower kinetic stability of the materials [35,36], however, it has been established that this conventional relation is not universally observed in all instances. The theoretical values of the energy gap of molecular orbital obtained from DFT calculation is represented in Table-4. Fig. 3 represents the HOMO-LUMO molecular surface plot for all the prepared compounds, from the figures it can be observed that in molecules **6a**, **6c**, **6e**, **6g**, **6i** and **6k** the HOMO density is spread over the quinoline linkage and quinazoline part of the molecule, hence in these molecules the obscure mobility of the electron around the R_1 substitution and R_2 substitution affects the intermolecular charge transfer while LUMO is delocalized over the whole quinoline ring with R_1, whereas in molecules **6b**, **6d**, **6f**, **6h**,**6j** and **6l**, the HOMO density is localized over quinoline nitrogen and the whole thiazole, quinazoline core spreading over the R_2 and R_3 substitution position, while the LUMO is delocalized over the quinoline ring, hence in such molecules the charge density on the benzothiazole ring allows

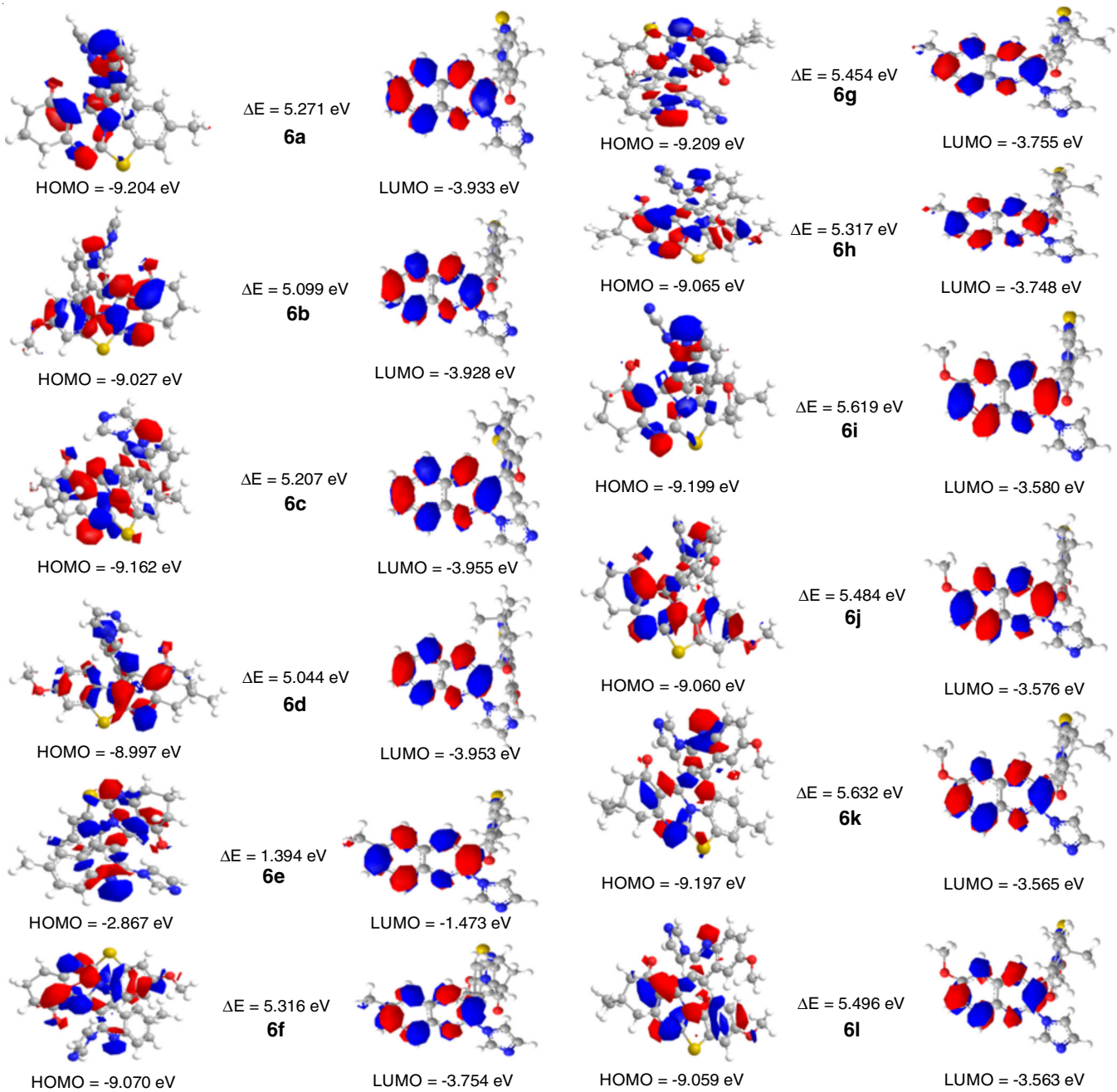

Fig. 3. Frontier molecular orbitals diagram of **6a-l**

it to bind with the protein with π-π and π-hydrogen interaction more firmly. Parameters based on the molecular orbital energy and their energy gap are also calculated where they can be used to relate them with other molecular properties of the ligand such parameters as softness, hardness, global softness, absolute softness, chemical potential, global electrophilicity, electronegativity and additional electronic charge are reported in Table-4 with the molecular energy, twist angles between planes and dipole moment. The relationship between ligand softness and biological activity has traditionally been acknowledged. However, based on the information shown in Table-4 and the corresponding biological activity statistics, it can be concluded that the results are insufficient for accurately predicting the reactivity of the molecules.

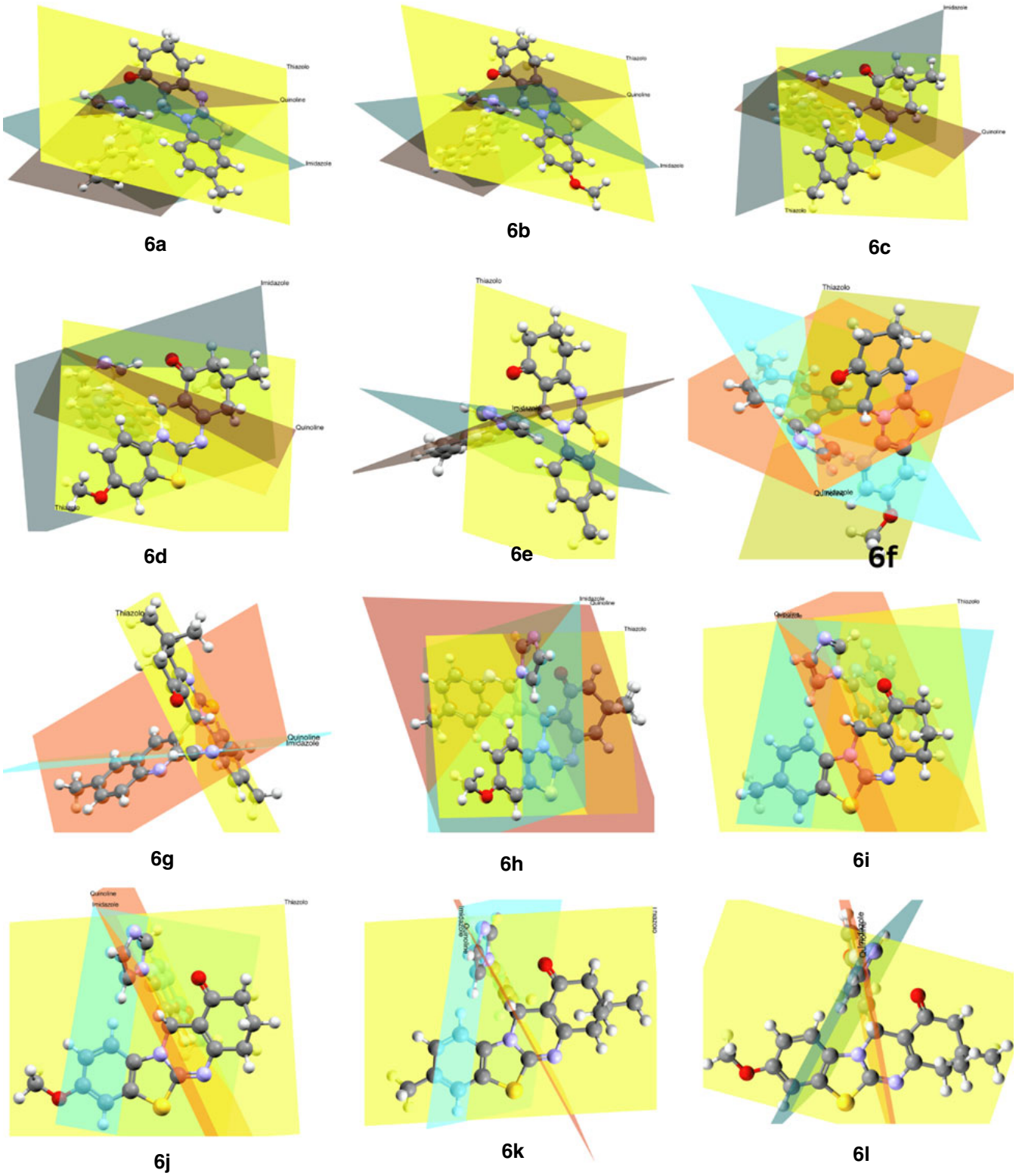

Fig. 4. Twist angle θ of **6a-l**

Molecular docking study: From the inhibition concentration data of EGFR kinase inhibition and antiproliferative activities (Table-1), it was observed that among all the prepared compounds, compound **6j** exhibited greater potency against all three cancer cell lines, which are EGFR, A549 and HepG2 with the IC_{50} of 0.14 ± 0.03, 2.24 ± 0.04 and 2.31 ± 0.04, respectively. Compound **6g** showed least activity against the EGFR with IC_{50} of 9.61 ± 0.11, while compound **6c** showed the least activity against A549 cell line with IC_{50} of 9.54 ± 0.12 and HepG2 IC_{50} of 11.27 ± 0.15, this can be attributed to the nature of the substituents in conjugation with the core of the molecule, the higher activity of the molecule can be due to the presence of alkoxy group at R_1 and R_3 positions as they can be a good hydrogen bond acceptor. While in the least active molecules the presence of CH_3 group at all the substitution position can only increase the electron density in the core, which must be binding with the pocket least firmly compared to the all other. The change in the substitution can affect the geometry of the molecule also which is a critical factor in protein binding and hence this change can bring a change in the twist angle between the aromatic part of the molecule allowing the molecule to fit perfectly or adversely in the pocket of the EFGR, which can be quantitatively, also qualitatively it can be observed in Fig. 4. The stronger biological interaction of compound **6j** with the protein are with residue LYS851 and ASN818, where it forms three hydrogen bonds, among which two hydrogen bonds were formed with LYS851, one was with the quinoline nitrogen and LYS with bond distance of 2.55 Å and the other one was between the π-electrons of imidazole ring and the LYS with bond distance of 2.81 Å, the third hydrogen bond was formed between the methoxy hydrogen and oxygen lone pair of ASN818 with bond distance of 3.31 Å with the binding energy of -6.8219 kcal/mol. These 2D and 3D interaction of compound **6j** with protein residues are shown in Fig. 5.

In case of FabH *E. coli* the inhibition concentration data for all the synthesized compounds shows that compound **6j** exhibited greater potency with the IC_{50} concentration of 3.1 µM, while compound **6a** showed the least potency against *E. coli* with the IC_{50} concentration of 17.5 µM, from the docking score it can be seen that compound **6j** bound with the least binding energy with the protein.

Conclusion

With the aim of synthesizing new molecules with biquinoline-imidazole-benzothiazole hybrids for their potential against lung and breast cancer, twelve derivatives were synthesized with small groups at substitution position. The synthesized series were aimed for their anticancer antimicrobial activity, where among prepared few significant biological results were obtained with a conclusion that when quinoline is present in the molecules, its nitrogen and the phenyl ring bind with the protein and enhances the binding with more affinity also, the quinoline-benzothiazole core with electron donating and H-bond acceptor plays a major role in fitting the active pocket of the protein. Compound **6j** was found to be the most active against EGFR, A549 and HepG2 cancer cell lines, while it was also found to be most active against FabH *E. coli*, although other members of the prepared series were also found to be active with comparatively higher inhibition concentration. The highest inhibition power of the potent prepared derivative against EGFR was about fourth time lower than the taken standard, while for A549 the potency was seventeenth time lower than the standard. To understand the binding posture and sites, molecular docking was performed. The DFT studies were also performed for these molecules to get the insight of structural parameters and their effect on the binding efficiently in the pocket by means of angle of the active part of the core allowing exposure o the receptor, distribution of charge density over the molecule responsible for the strength of hydrogen bonding and π-π interaction strength, resulting in the optimization of the binding affinity. From this study and observation, it can be concluded that molecules with quinoline and broader molecular core composed of quinoline-benzothiazole pharmacophores can be used as templet and can be further structurally modified for target-based application, evaluating the further scope of the pharmacophore and study the limitations that cannot be explored by *in vitro* is further needed.

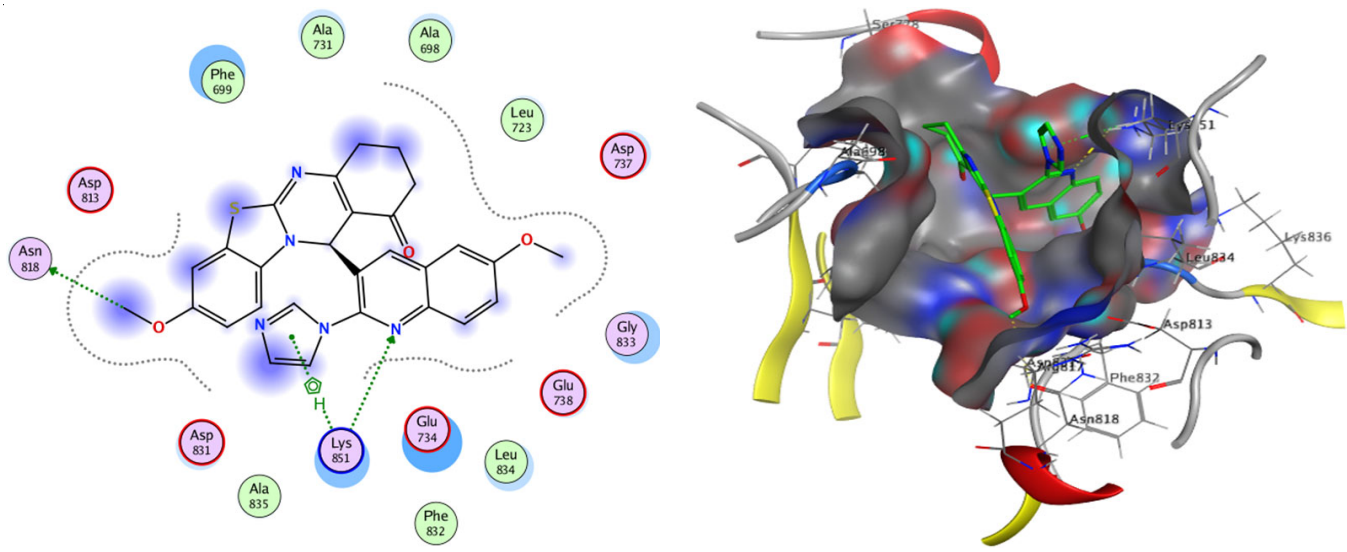

Fig. 5. 2D and 3D Binding model of compound **6j** into the active pocket of EGFR

ACKNOWLEDGEMENTS

The authors are thankful to Shri Maneklal M. Patel Institute of Sciences and Research, Kadi Sarva Vishwavidhyalaya for giving research and laboratory facilities.

CONFLICT OF INTEREST

The authors declare that there is no conflict of interests regarding the publication of this article.

REFERENCES

1. T.S. Ibrahim, M.M. Hawwas, E. Taher, N.A. Alhakamy, M.A. Alfaleh, M. Elagawany, B. Elgendy, G.M. Zayed, M.F.A. Mohamed, Z.K. Abdel-Samii and Y.A.M.M. Elshaier, *Bioorg. Chem.*, **105**, 104352 (2020); https://doi.org/10.1016/j.bioorg.2020.104352
2. R.L. Siegel, K.D. Miller, H.E. Fuchs and A. Jemal, *CA Cancer J. Clin.*, **71**, 7 (2021); https://doi.org/10.3322/caac.21654
3. M. Morales-Cruz, Y. Delgado, B. Castillo, C.M. Figueroa, A.M. Molina, A. Torres, M. Milián and K. Griebenow, *Drug Des. Devel. Ther.*, **13**, 3753 (2019); https://doi.org/10.2147/DDDT.S219489
4. M. Tateishi and T. Ishida, *Cancer Res.*, **50**, 7077 (1990).
5. A. Ayati, S. Moghimi, S. Salarinejad, M. Safavi, B. Pouramiri and A. Foroumadi, *Bioorg. Chem.*, **99**, 103811 (2020); https://doi.org/10.1016/j.bioorg.2020.103811
6. P. Wee and Z. Wang, *Cancers*, **9**, 52 (2017); https://doi.org/10.3390/cancers9050052
7. K.S. Kolibaba and B.J. Druker, *Biochim. Biophys. Acta*, **1333**, F217 (1997); https://doi.org/10.1016/s0304-419x(97)00022-x
8. E.J. Meuillet and E.G. Bremer, *Pediatr. Neurosurg.*, **29**, 1 (1998); https://doi.org/10.1159/000028677
9. L.V. Sequist, *Oncologist*, **12**, 325 (2007); https://doi.org/10.1634/theoncologist.12-3-325
10. L. Serwecinska, *Water*, **12**, 3313 (2020); https://doi.org/10.3390/w12123313
11. X. Wen, S.-B. Wang, D.-C. Liu, G.-H. Gong and Z.-S. Quan, *Med. Chem. Res.*; **24**, 2591 (2015); https://doi.org/10.1007/s00044-015-1323-y
12. R. Kaur and K. Kumar, *Eur. J. Med. Chem.*, **215**, 113220 (2021); https://doi.org/10.1016/j.ejmech.2021.113220
13. F. Zhang, Q. Wen, S.-F. Wang, B. Shahla Karim, Y.-S. Yang, J.-J. Liu, W.-M. Zhang and H.-L. Zhu, *Bioorg. Med. Chem. Lett.*, **24**, 90 (2013); https://doi.org/10.1016/j.bmcl.2013.11.079
14. S.W. White, J. Zheng, Y.M. Zhang and C.O. Rock, *Annu. Rev. Biochem.*, **74**, 791 (2005); https://doi.org/10.1146/annurev.biochem.74.082803.133524
15. Y.-J. Lu, Y.-M. Zhang and C.O. Rock, *Biochem. Cell Biol.*, **82**, 145 (2004); https://doi.org/10.1139/o03-076
16. M. Chen and J. Huang, *Precis. Clin. Med.*, **2**, 183 (2019); https://doi.org/10.1093/pcmedi/pbz017
17. Y.-T. Wang, T.-Q. Shi, J. Fu and H.-L. Zhu, *Eur. J. Med. Chem.*, **171**, 209 (2019); https://doi.org/10.1016/j.ejmech.2019.03.026
18. K.S. Gajiwala, S. Margosiak, J. Lu, J. Cortez, Y. Su, Z. Nie and K. Appelt, *FEBS Lett.*, **583**, 2939 (2009); https://doi.org/10.1016/j.febslet.2009.08.001
19. M. Negi, P.A. Chawla, A. Faruk and V. Chawla, *Bioorg. Chem.*, **104**, 104315 (2020); https://doi.org/10.1016/j.bioorg.2020.104315
20. A. Mermer, T. Keles and Y. Sirin, *Bioorg. Chem.*, **114**, 105076 (2021); https://doi.org/10.1016/j.bioorg.2021.105076
21. P. Yadav and K. Shah, *Bioorg. Chem.*, **109**, 104639 (2021); https://doi.org/10.1016/j.bioorg.2021.104639
22. J. Drogosz-Stachowicz, A. Dlugosz-Pokorska, K. Gach-Janczak, A. Jaskulska, T. Janecki and A. Janecka, *Chem. Biol. Interact.*, **320**, 109005 (2020); https://doi.org/10.1016/j.cbi.2020.109005
23. K.D. Katariya, S.R. Shah and D. Reddy, *Bioorg. Chem.*, **94**, 103406 (2019); https://doi.org/10.1016/j.bioorg.2019.103406
24. R. Musiol, *Expert Opin. Drug Discov.*, **12**, 583 (2017); https://doi.org/10.1080/17460441.2017.1319357
25. M.C. Mandewale, U.C. Patil, S.V. Shedge, U.R. Dappadwad and R.S. Yamgar, *Beni. Suef Univ. J. Basic Appl. Sci.*, **6**, 354 (2017); https://doi.org/10.1016/j.bjbas.2017.07.005
26. P. Teng, C. Li, Z. Peng, V. Anne Marie, A. Nimmagadda, M. Su, Y. Li, X. Sun and J. Cai, *Bioorg. Med. Chem.*, **26**, 3573 (2018); https://doi.org/10.1016/j.bmc.2018.05.031
27. Z. Xiao, F. Lei, X. Chen, X. Wang, L. Cao, K. Ye, W. Zhu and S. Xu, *Arch. Pharm.*, **351**, 1700407 (2018); https://doi.org/10.1002/ardp.201700407
28. D. Mantu, V. Antoci, C. Moldoveanu, G. Zbancioc and I.I. Mangalagiu, *J. Enzyme Inhib. Med. Chem.*, **31(S2)**, 96 (2016); https://doi.org/10.1080/14756366.2016.1190711
29. A. Irfan, F. Batool, S.A. Zahra Naqvi, A. Islam, S.M. Osman, A. Nocentini, S.A. Alissa and C.T. Supuran, *J. Enzyme Inhib. Med. Chem.*, **35**, 265 (2020); https://doi.org/10.1080/14756366.2019.1698036
30. M. Haroun, C. Tratrat, K. Kositzi, E. Tsolaki, A. Petrou, B. Aldhubiab, M. Attimarad, A. Geronikaki, K.N. Venugopala, H.S. Elsewedy, S. Harsha, M. Sokovic, J. Glamoclija and A. Ciric, *Curr. Top. Med. Chem.*, **18**, 75 (2018); https://doi.org/10.2174/1568026618666180206101814
31. N.C. Desai, D. Pandya and D. Vaja, *Med. Chem. Res.*, **27**, 52 (2018); https://doi.org/10.1007/s00044-017-2040-5
32. A. Singh, A. Pandurangan, K. Rana, P. Anand, A. Ahamad and A.K. Tiwari, *Int. Curr. Pharm. J.*, **1**, 110 (2012); https://doi.org/10.3329/icpj.v1i5.10284
33. R. Ali and N. Siddiqui, *J. Chem.*, **2013**, 345198 (2013); https://doi.org/10.1155/2013/345198
34. F. Neese, *Wiley Interdiscip. Rev. Comput. Mol. Sci.*, **12**, e1606 (2022); https://doi.org/10.1002/wcms.1606
35. R. Kurtaran, S. Odabasioglu, A. Azizoglu, H. Kara and O. Atakol, *Polyhedron*, **26**, 5069 (2007); https://doi.org/10.1016/j.poly.2007.07.021
36. W.H. Mahmoud, M.M. Omar, F.N. Sayed and G.G. Mohamed, *Appl. Organomet. Chem.*, **32**, 4386 (2018); https://doi.org/10.1002/aoc.4386